ALTERED MERISTEM PROGRAM1 Restricts Shoot Meristem Proliferation and Regeneration by Limiting HD-ZIP III-Mediated Expression of RAP2.6L[1][OPEN]

Saiqi Yang, Olena Poretska, and Tobias Sieberer[2]

Research Unit Plant Growth Regulation, Department of Plant Sciences, Technical University of Munich, Weihenstephan, DE-85354 Freising, Germany

ORCID IDs: 0000-0002-6425-3731 (S.Y.); 0000-0002-4462-9260 (T.S.)

Plants show an indeterminate mode of growth by the activity of organ forming stem cell niches in apically positioned meristems. The correct formation and activity of these meristems are a prerequisite for their adaptive development and also allow the maintenance of organogenesis under adverse circumstances such as wounding. Mutation of the putative Arabidopsis (*Arabidopsis thaliana*) Glu carboxypeptidase ALTERED MERISTEM PROGRAM1 (AMP1) results in Arabidopsis plants with enlarged shoot apical meristems, supernumerary stem cell pools, and higher leaf formation rate. AMP1 deficiency also causes exaggerated de novo formation of shoot meristems. The activity of AMP1 has been implicated in the control of microRNA (miRNA)-dependent translation; however, it is not known how this function contributes to the shoot meristem defects. Here, we show that the transcription factor RAP2.6L is upregulated in the Arabidopsis *amp1* mutant. Overexpression of RAP2.6L in the wild type causes *amp1* mutant-related phenotypic and molecular defects, including enhanced shoot regeneration in tissue culture. Conversely, inhibition of RAP2.6L in the *amp1* mutant suppresses stem cell hypertrophy and the regenerative capacity. We further provide evidence that *RAP2.6L* is under direct transcriptional control of miRNA-regulated class III homeodomain-Leu zipper (HD-ZIP III) proteins, key regulators of shoot meristem development, which overaccumulate in the *amp1* mutant. Our results reveal a transcription factor module acting downstream of *AMP1* in the control of shoot stem cell niche patterning. By positioning the HD-ZIP III/RAP2.6L module downstream of AMP1 function, we provide a mechanistic link between the role of AMP1 in miRNA-mediated translational repression and shoot stem cell specification.

A key requirement for morphogenesis and tissue homeostasis in multicellular organisms is the correct spatiotemporal control of differentiation in the progeny of stem cell populations. Disturbances in this process cause developmental and regenerative defects and are also the basis for cancerous transformation. Plants harbor stem cell niches (SCNs) in apical meristems, which are responsible for the continuous formation of new organs during postembryonic development. This indeterminate mode of growth allows plants to steadily uptake resources and adapt to prevailing environmental conditions. The dome-shaped shoot apical meristem (SAM), which is the source of all shoot organs, consists of different functional zones. Stem cells in the central zone give rise to daughter cells, which undergo transition to a determinate cell fate during the process of organ initiation in the ring-like periphery, called the morphogenetic zone (Sluis and Hake, 2015). Maintenance of this spatial organization is a prerequisite for meristem function and requires the formation of cell identity borders through feedback-regulated communication events (Gaillochet and Lohmann, 2015). Comprehensive characterization of the underlying signaling not only contributes to a mechanistic understanding of plant organogenesis but might also unveil molecular targets to optimize yield traits in crop species (Je et al., 2016).

The stem cell niche in the shoot meristem consists of an apical stem cell pool and an underlying organizing center (OC). The identity of the OC is specified by the expression of the homeodomain transcription factor *WUSCHEL* (*WUS*; Mayer et al., 1998). WUS enters the stem cells by symplastic movement to maintain their identity as well as to activate the transcription of *CLV3* (Yadav et al., 2011; Daum et al., 2014). The peptide CLV3 in turn diffuses back to more basal regions of the meristem and limits lateral expansion of *WUS* expression (Brand et al., 2000; Schoof et al., 2000). The position of the WUS expression domain is determined by the establishment of a local response maximum for the

[1]This work was supported by the Austrian Science Fund (P19935 to T.S.), by an APART fellowship from the Austrian Academy of Sciences (11300 to T.S.), by the German Federal Ministry of Education and Research (031A327 and 031B0554 to T.S.), and by a PhD fellowship from the China Scholarship Council (to S.Y.). S.Y. was a member of the Technical University of Munich Graduate School.

[2]Address correspondence to tobias.sieberer@wzw.tum.de.

The author responsible for distribution of materials integral to the findings presented in this article in accordance with the policy described in the Instructions for Authors (www.plantphysiol.org) is: Tobias Sieberer (tobias.sieberer@wzw.tum.de).

T.S. conceived the experiments; O.P. performed the hyperphyllin treatments and precursory microarray experiments; S.Y. performed all other experiments; S.Y. and T.S. analyzed and interpreted the data; S.Y. and T.S. wrote the manuscript.

[OPEN]Articles can be viewed without a subscription.

www.plantphysiol.org/cgi/doi/10.1104/pp.18.00252

hormone cytokinin (Gordon et al., 2009; Chickarmane et al., 2012). Multilayered feedback control between cytokinin, WUS, and CLV3 thus guarantees the dynamic repositioning and size adjustment of the SCN in the shoot meristem (Gaillochet and Lohmann, 2015).

Upon entering the peripheral zone, stem cell descendants undergo transient proliferation and are subsequently incorporated into organ primordia. Suppression of stemness in these cells is a key prerequisite to maintaining the radial integrity of the meristem and is mediated by epigenetic mechanisms since mutants in chromatin assembly and remodeling have been shown to display reactivation of stem cell markers in the morphogenetic zone (Gaillochet and Lohmann, 2015). This process also requires active signaling from the existing SCN as elimination of the primary OC results in the formation of secondary SCNs in the meristem periphery (Loiseau, 1959; Reinhardt et al., 2003). However, the molecular basis of this lateral inhibition mechanism is not known. There is growing evidence that class III homeodomain-Leu zipper (HD-ZIP III) transcription factors contribute to the radial organization of the SAM. HD-ZIP III proteins define apical central identity and proper shoot SCN positioning in the embryo (Roodbarkelari and Groot, 2017) and altered HD-ZIP III activity causes the formation of ectopic stem cell pools in the shoot meristem periphery (Green et al., 2005; Williams et al., 2005; Kim et al., 2008). The function of HD-ZIP III proteins is controlled at several regulatory levels by micro RNAs (miRNAs), microProteins, and potentially also unidentified small molecule signals (Roodbarkelari and Groot, 2017). Moreover, their activity is also modulated by heterodimerization between family members and interaction with other transcription factors (Chandler et al., 2007; Magnani and Barton, 2011). This high level of functional connectivity predestines HD-ZIP IIIs as convergence hubs to integrate spatiotemporal information in the process of SAM patterning. However, how they execute this role at the molecular level is not well known.

Another key regulator of radial SAM organization is the putative Glu carboxypeptidase ALTERED MERISTEM PROGRAM1 (AMP1; Helliwell et al., 2001). Inactivation of this enzyme causes vegetative SAM enlargement and an increased leaf formation rate, which originate at least partially from a strong tendency to generate ectopic SCNs in the SAM periphery (Huang et al., 2015). The observed disintegration of the radial SAM in the Arabidopsis (*Arabidopsis thaliana*) *amp1* mutant could not be attributed to the enhanced cytokinin synthesis found in the mutant and indicated the involvement of a cytokinin-independent mechanism (Huang et al., 2015). Although the biochemical function of AMP1 is not known, it was recently shown to be required for miRNA-mediated translational inhibition at the rough endoplasmic reticulum (Li et al., 2013). However, whether the radial formation of ectopic SCNs in the *amp1* mutant is the consequence of overtranslation of miRNA targets involved in SAM control, such as HD-ZIP III transcription factors, remains to be tested.

A key function of AMP1 in the suppression of shoot stem cell identity is also underlined by the high de novo shoot formation capacity of AMP1-defective plants (Chaudhury et al., 1993). Shoot regeneration in tissue culture usually implicates the formation of pluripotent callus cells in explants on auxin-rich callus-induction medium. Callus cells, which have root meristem-like identity, transdifferentiate into WUS-expressing foci on cytokinin-rich shoot induction medium, which subsequently establish functional shoot meristems (Ikeuchi et al., 2016). A number of transcription factors that mediate this transdifferentiation process have been identified, including HD-ZIP III proteins (Kareem et al., 2016). A point mutation affecting the MEHKLA domain of ATHB15/CORONA was reported to trigger shoot regeneration in a cytokinin-independent manner (Duclercq et al., 2011a), and HD-ZIP IIIs directly activate WUS expression in a complex with B-type ARABIDOPSIS RESPONSE REGULATORs during de novo SAM formation (Zhang et al., 2017). Transcription factors belonging to the APETALA2/Ethylene Responsive Factor (AP2/ERF) family also play a prominent role in this process (Ikeuchi et al., 2016). Whereas ENHANCER OF SHOOT REGENERATION1/DORNRÖSCHEN (ESR1/DRN) and ESR2/DRN-LIKE (DRNL) are activated by and subsequently mediate the cytokinin effect (Banno et al., 2001; Matsuo et al., 2011), RAP2.6L has been shown to be required for shoot regeneration in tissue culture without being transcriptionally regulated by cytokinin under these conditions (Che et al., 2006).

To better understand the function of AMP1 in SCN establishment, we screened transcriptome data of the *amp1* mutant for potential components acting downstream of the enzyme and identified *RAP2.6L* to be strongly upregulated in the mutant. Ectopic expression of *RAP2.6L* in the wild type caused mild *amp1*-related SAM phenotypes, including an increased meristem size, an elevated leaf formation rate, and altered expression of SAM markers, whereas perturbation of RAP2.6L function in the *amp1* mutant suppressed the SAM hypertrophy as well as the increased shoot regeneration capacity. We further show that RAP2.6L is transcriptionally controlled by HD-ZIP III proteins, which directly bind to the RAP2.6L promoter. Based on our findings, we present a model in which AMP1 limits SAM activity by constraining the expression of *RAP2.6L* through miRNA-dependent translational control of HD-ZIPIII transcription factors.

RESULTS

Expression of *RAP2.6L* Is Upregulated in the *amp1* Mutant

In an effort to better understand the molecular role of AMP1 in shoot meristem function, we screened our recently published *amp1* transcriptome data for

misregulated factors reported to play a role in SAM patterning and/or activity (Poretska et al., 2016). In this analysis, we found the AP2/ERF transcription factor RAP2.6L to be significantly upregulated in the *amp1-13* mutant compared to wild type. Since RAP2.6L is required for shoot regeneration (Che et al., 2006) and the *amp1* mutant shows ectopic OC formation in the shoot meristem periphery (Huang et al., 2015), we further investigated the functional relationship between these two factors. To confirm the altered expression of *RAP2.6L* in the *amp1* mutant, we performed reverse transcription-quantitative PCR (qPCR) analysis in the *amp1-13* mutant and the *amp1 lamp1* double mutant, in which the putative paralog *LIKE-AMP1* (*LAMP1*) is also mutated. *RAP2.6L* was strongly upregulated in the *amp1-13* and *amp1-1 lamp1-2* mutants compared to the wild-type Col-0 (Fig. 1A). Similarly, significantly enhanced expression of *RAP2.6L* was detected in L*er* plants bearing the *amp1* allele *primordia timing* (*pt*; Fig. 1A). Of the closest paralogs of RAP2.6L in the ERF-TF subfamily group X, the transcript levels of RAP2.6 (in the *amp1-13* and *pt* mutants) and ERF112 (in the *amp1-13* mutant) were slightly elevated in the *amp1* mutant background; however, these changes were not significant under our experimental conditions. (Supplemental Fig. S1, A and B).

To examine the enhanced expression levels of *RAP2.6L* in the *amp1* mutant at the tissue level, we created the transcriptional GUS reporter *pRAP2.6L::GUS*. Similar to the *RAP2.6L promoter:GUS* line (Che et al., 2006), our reporter showed the strongest activity in the shoot apex, the hypocotyl, and the vascular tissues of wild-type seedlings (Fig. 1B), with the single exception that it did not noticeably display the reported expression front in young leaf primordia connected to leaf maturation processes (Che et al., 2006). In 8-d-old *amp1-1* seedlings, *pRAP2.6L::GUS* activity was generally enhanced with the strongest alteration in young leaf primordia, whereas staining was barely visible in the wild-type background (Fig. 1B). This pronounced expression of *RAP2.6L* in *amp1* shoot apices and vascular tissues was already detectable directly after germination in 4-d-old seedlings (Fig. 1B). The elevated transcript levels of *RAP2.6L* in the *amp1* mutant also resulted in an overaccumulation of RAP2.6L since we found a higher activity of *pRAP2.6L::RAP2.6L-GUS* (Krishnaswamy et al., 2011) in the mutant background compared to the wild type (Fig. 1C). The weak activity of this reporter was only detectable in the areas of strongest expression of the transcriptional *pRAP2.6L::GUS* reporter, including vascular tissues around the SAM and the base of young leaf primordia. Finally, consistent with an AMP1-dependent control of *RAP2.6L* expression, *pRAP2.6L::GUS* activity in the wild type was also induced after treatment with the chemical hyperphyllin (Fig. 1D), which causes *amp1*-related phenotypic and molecular defects (Poretska et al., 2016).

To test whether the augmented expression of *RAP2.6L* is caused by the enhanced cytokinin levels previously reported in the *amp1* mutant (Nogué et al., 2000), we analyzed the response of *pRAP2.6L::GUS* activity to short- and long-term treatments with *trans*-zeatin. None of these exogenous cytokinin treatments affected the *pRAP2.6L::GUS* staining pattern or intensity in either the wild type or the *amp1-1* mutant (Supplemental Fig. S2), indicating that the pronounced expression of *RAP2.6L* in the *amp1* mutant is not caused by the altered homeostasis of this hormone. Taken together, RAP2.6L shows increased and partially ectopic expression in the *amp1* mutant in a cytokinin-independent manner, and this altered expression is most prominent in shoot tissues with high *AMP1* expression levels such as young leaf primordia (Vidaurre et al., 2007).

Overexpression of *RAP2.6L* Causes *amp1*-Related Shoot Phenotypes

To investigate whether the enhanced expression of *RAP2.6L* in the *amp1* mutant contributes to any of the mutant SAM phenotypes, we analyzed shoot meristem activity parameters in the *35S::RAP2.6L* plants (named *RAP2.6L-OX* throughout this study; Krishnaswamy et al., 2011) grown under short-day conditions. In this line, an obvious increase in true leaf formation became apparent from day 20 on (Fig. 2, A and B). Since the elevated leaf formation in the *amp1* mutant correlates with the presence of a hypertrophic SAM, we assessed the meristem dimensions of *RAP2.6L-OX* seedlings. *RAP2.6L-OX* SAMs displayed a larger surface area (Fig. 2C) as well as an increased lateral and distal expansion in median longitudinal sections (Fig. 2, D and E). The observed increase in the size of the SAM correlated with enlargement of the OC domain (*pWUS::GUS*; Fig. 2F) as well as the stem cell pool (*pCLV3::GUS*; Fig. 2F), which is in its extent comparable to that of early developmental stages of weak *amp1* mutant alleles (Huang et al., 2015). Moreover, expression of the mitotic *CYCLIN B1;1 (CYCB1;1)::GUS* reporter was increased in the shoot meristematic area and in young leaf primordia of the *RAP2.6L-OX* plants (Fig. 2F), as was found in the faster-forming leaves of the *amp1* mutant (Poretska et al., 2016). Notably, we also observed in the *RAP2.6L-OX* plants a significantly broadened activity of *pKLU::GUS*, a reporter for the SAM boundary marker CYP78A5/KLUH (Fig. 2F), which controls the rate of leaf formation (Wang et al., 2008) and was prominently upregulated in the *amp1* mutant (Helliwell et al., 2001; Griffiths et al., 2011; Poretska et al., 2016).

As previously described (Krishnaswamy et al., 2011), *RAP2.6L* overexpression also provoked a significant reduction in flowering time under long-day conditions, another developmental defect shared with the *amp1-1* mutant (Fig. 3A). Moreover, both genotypes underwent floral transition under noninductive short-day conditions in a temporal window of 20 to 27 d after germination (DAG), whereas wild-type plants did not flower under these conditions even at 86 DAG (Fig. 3, A and B). They also produced similar inflorescence structures with a higher number of cauline branches

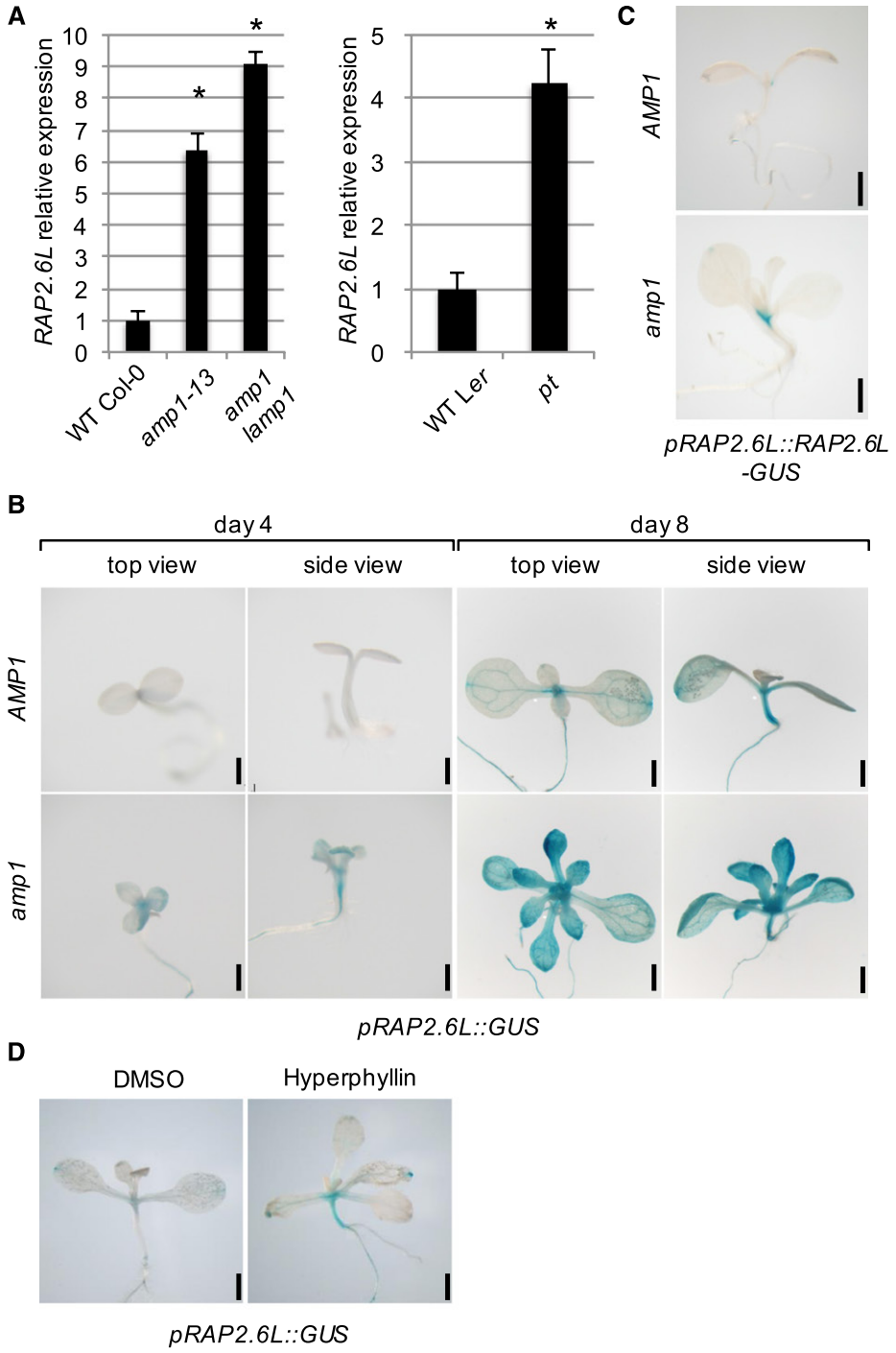

Figure 1. *RAP2.6L* expression is upregulated in *amp1*. A, qPCR analysis of *RAP2.6L* expression in 8-d-old seedlings of the indicated lines. Fold changes compared to the respective wild-type (WT) are shown. Error bars indicate the SE calculated from three biological replicates (at least 30 seedlings per replicate; replicates were grown at the same time on different petri dishes) after normalization to *UBIQUITIN-CONJUGATING ENZYME* (*UBC*). Asterisks indicate a significant difference (Student's two-tailed *t* test; $P < 0.05$). B, *pRAP2.6L::GUS* activity in wild-type Col-0 (WT) and the *amp1-1* mutant at 4 and 8 DAG. C, *pRAP2.6L::RAP2.6L-GUS* activity in wild-type Col-0 (WT) and the *amp1-1* mutant at 8 DAG. D, *pRAP2.6L::GUS* activity in 10-d-old wild-type Col-0 seedlings grown in liquid medium containing either 0.5% DMSO (mock) or 30 μM hyperphyllin. Bars = 1 mm (B–D).

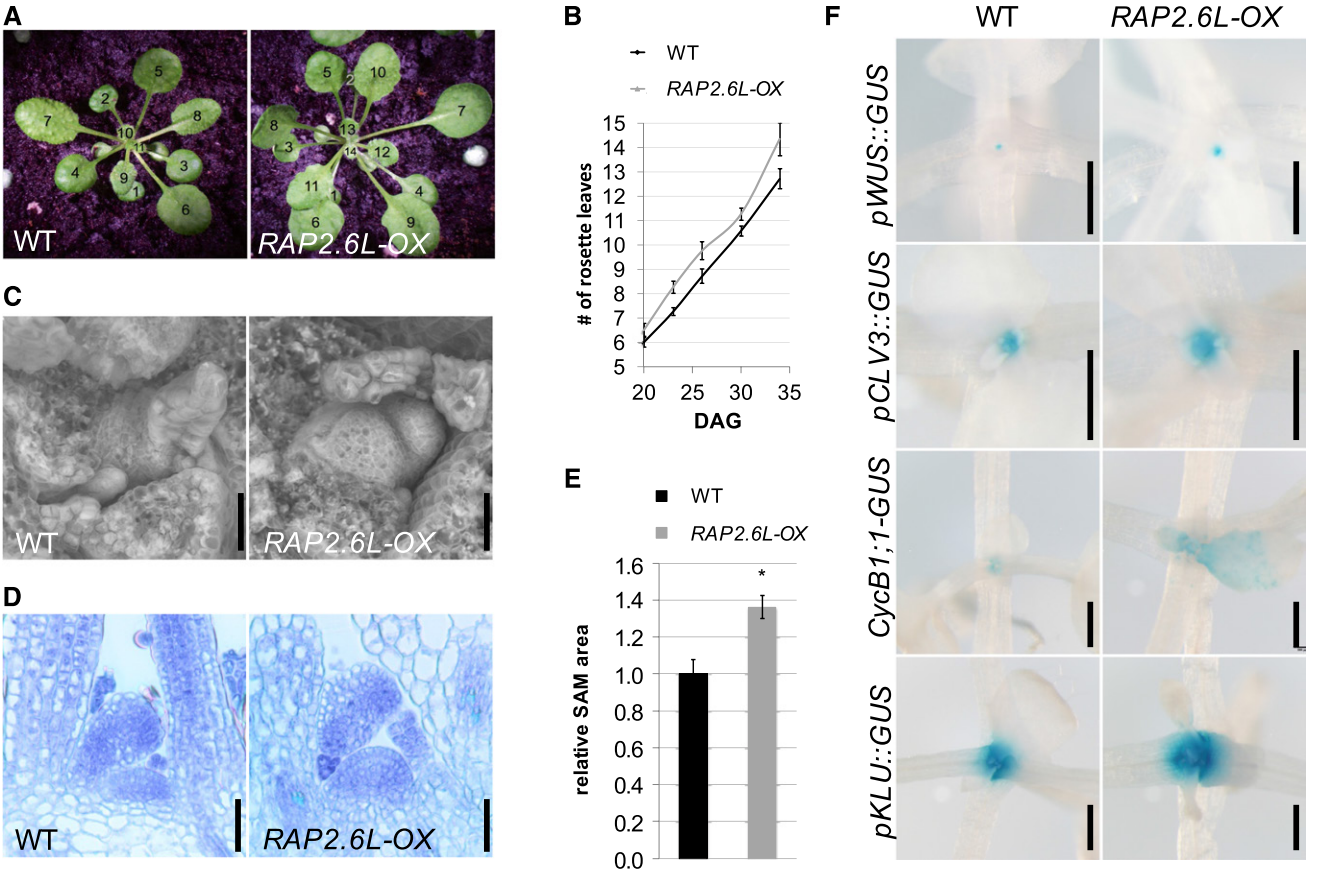

Figure 2. *RAP2.6L-OX* plants show *amp1*-related vegetative phenotypes. A, Wild-type Col-0 (WT) and *RAP2.6L-OX* plants grown under short-day conditions for 34 d. Leaves are numbered in the consecutive order of appearance. B, Quantification of rosette leaves in wild-type Col-0 (WT) and *RAP2.6L-OX* plants at the indicated time points grown under short-day conditions (values represent means ± SE; $n \geq 8$). C, Scanning electron micrographs of SAM areas of wild-type Col-0 (WT) and *RAP2.6L-OX* seedlings grown under short-day conditions for 18 d. D, Median longitudinal SAM sections of wild-type Col-0 (WT) and *RAP2.6L-OX* seedlings grown under short-day conditions for 18 d. E, Quantification of SAM area from median longitudinal sections of wild-type Col-0 (WT) and *RAP2.6L-OX* seedlings. Normalized values (wild type = 1) are shown (bars represent means ± SE; $n \geq 3$). Asterisk indicates a significant difference (Student's two-tailed *t* test; $P < 0.05$). F, Comparison of GUS activities of the indicated reporter lines in wild-type and *RAP2.6L-OX* seedlings grown under short-day conditions. Plants were analyzed at 15 DAG except for pWUS::GUS (18 DAG). Bars = 25 µm (C and D) and 500 µm (F).

and flower formations starting at a closer distance to the rosette compared to the wild type (Fig. 3, B and C). We conclude that ectopic expression of *RAP2.6L* causes mild *amp1*-like phenotypic and molecular alterations in vegetative SAM activity, flowering time, and inflorescence architecture.

Compromised RAP2.6L Function Suppresses the Enhanced Leaf Formation Rate of the *amp1* Mutant

Since the expression of *RAP2.6L* is deregulated in the *amp1* mutant and the *RAP2.6L-OX* and *amp1* plants share similar defects in shoot development, one mode of how AMP1 could restrain SAM activity might be through spatial or temporal limitation of RAP2.6L expression. To this end, we investigated the effect of inactivation of RAP2.6L as well as inactivation of its closest paralogs on shoot meristem function in the wild type and the *amp1* mutant. For this purpose, we used T-DNA insertion lines, which were available for *RAP2.6L*, *RAP2.6*, and *ERF112* (Che et al., 2006). In addition, the transcriptional repression domain SUPERMAN Repression Domain X (SRDX) and the *MYC* epitope tag were fused to the 35S-driven open reading frames (ORFs) of RAP2.6L and ERF BUD ENHANCER (EBE), resulting in the transgenic lines *RAP2.6L-SX* and *EBE-SX*, respectively. Except for a slightly retarded outgrowth of the first pair of true leaves in the loss-of-function single mutant of *RAP2.6L*, the *rap2.6l*, *rap2.6*, and *erf112* single mutants did not show a measurable impact on leaf formation in the wild-type or *amp1* background (Fig. 4, A and B; Supplemental Fig. S3, A and B). We found a suppressive effect of the *rap2.6l erf112* double mutation on the enhanced leaf formation rate of the *amp1* mutant in 7-d-old seedlings (Fig. 4, A and B), which disappeared again in later developmental stages

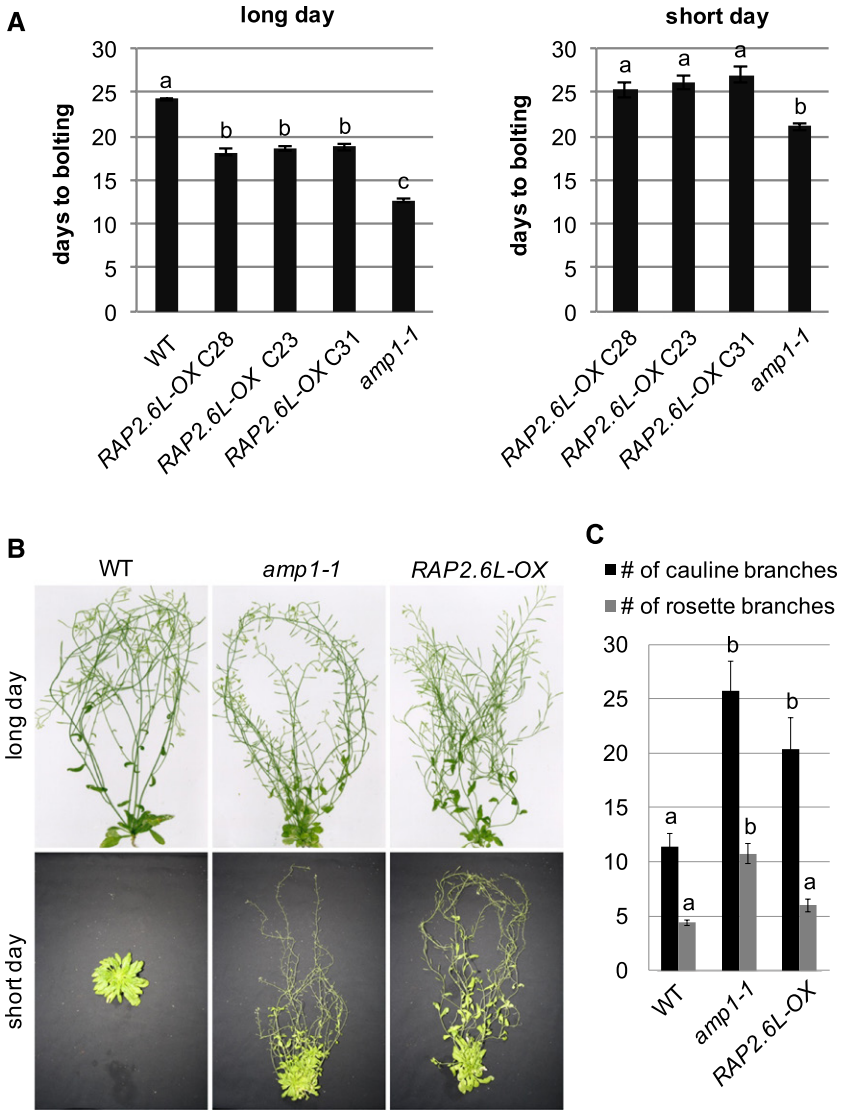

Figure 3. *RAP2.6L-OX* plants show *amp1*-related adult phenotypes. A, Quantification of flowering time of the indicated genotypes grown under long-day (left) and short-day conditions (right; wild type not shown since it did not flower in the analyzed period of time). Bars show means ± SE; $n \geq 15$. Different letters over the error bars indicate significant differences ($P < 0.05$) as calculated by Duncan's multiple range test. B, Comparison of wild-type Col-0 (WT), *amp1-1*, and *RAP2.6L-OX* shoots grown under long-day (70 DAG) or short-day (86 DAG) conditions. C, Quantification of the rosette branch number and cauline branch number of 70-d-old wild-type Col-0 (WT), *amp1-1*, and *RAP2.6L-OX* plants grown under long-day conditions (bars represent means ± SE; $n \geq 4$). Different letters over the error bars indicate significant differences ($P < 0.05$) as calculated by Duncan's multiple range test.

(Fig. 4, C and D), whereas the *rap2.6l rap2.6* double mutant was aphenotypic in this respect (Supplemental Fig. S3, A and B). The *RAP2.6L-SX* transgene was even more potent in rescuing the enhanced leaf production of the *amp1* mutant at 7 DAG, and this effect persisted throughout the vegetative growth phase. Notably, the relative suppression in leaf number by the RAP2.6L-SX activity was stronger in the *amp1* background (7 DAG, 52%; 12 DAG, 36%) than in the wild-type background (7 DAG, 32%; 12 DAG, 27%), supporting a specific genetic interaction rather than an independent effect (Supplemental Fig. S4). Furthermore, although the *EBE-SX* transgene also affected the leaf formation rate in the wild-type background with increasing efficiency during development, its suppressive effect on the *amp1* background was only marginal (Fig. 4, A–D). Taken together, these data suggest that deregulated expression of *RAP2.6L* in the *amp1* mutant contributes to its shortened plastochron.

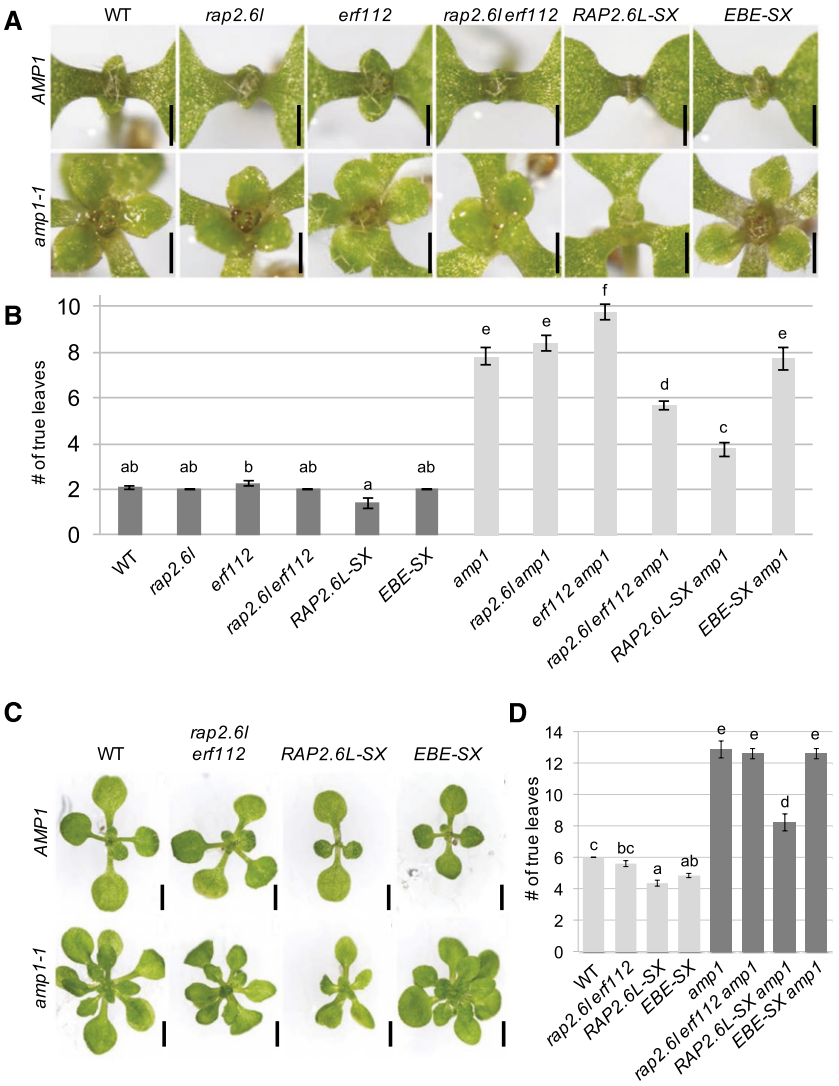

Figure 4. Compromised function of RAP2.6L suppresses the enhanced leaf formation rate of the *amp1* mutant. A, Shoot apices of Col-0 (WT), *rap2.6l-1*, *erf112-1*, *rap2.6l-1 erf112-1*, *RAP2.6L-SX*, and *EBE-SX* seedlings in the wild-type background at 7 DAG (top). Shoot apices of the same lines in the *amp1-1* background at 7 DAG (bottom). B, Quantification of the number of true leaves of the indicated genotypes at 7 DAG (bars represent means ± SE; $n \geq 10$). Bars for plant lines in the wild-type background are colored in dark gray, and bars for lines in the *amp1-1* background are colored in light gray. Different letters over the error bars indicate significant differences ($P < 0.05$) as estimated by Duncan's multiple range test. C, Comparison of Col-0 (WT), *rap2.6l-1 erf112-1*, *RAP2.6L-SX*, and *EBE-SX* seedlings in the wild-type background at 12 DAG (top) and seedlings of the same lines in the *amp1-1* background at 12 DAG (bottom). D, Quantification of the number of true leaves of the indicated genotypes at 12 DAG (bars represent means ± SE; $n \geq 8$). Bars for plant lines in the wild-type background are colored in light gray, and bars for lines in the *amp1-1* background are colored in dark gray. Different letters over the error bars indicate significant differences ($P < 0.05$) as estimated by Duncan's multiple range test. Bars = 500 µm (A) and 2 mm (C).

Compromised Function of RAP2.6L Minimizes Overproliferation of the SAM in the *amp1* Mutant

To investigate whether the SAM expansion phenotype of the *amp1* mutant is also specifically affected by perturbation of the function of RAP2.6L, we analyzed the SAM structures in the generated lines. Determination of the SAM area in median longitudinal shoot sections revealed that all lines except for *erf112* showed a slight but not significant reduction in meristem size when in the wild-type background (Fig. 5, A and B). In contrast, the presence of the *RAP2.6L-SX* transgene reduced the size of the SAM in the *amp1* mutant by over 50%. We also found significant, yet less pronounced, suppression of the size of the *amp1* mutant SAM in the *rap2.6l* and *rap2.6l erf112* mutants and in the presence of the *EBE-SX* transgene, whereas the mutation in *erf112* was again ineffective in this respect (Fig. 5C). The striking suppressive impact of the RAP2.6L-SX transgene on the meristematic overproliferation of the

amp1 mutant was also reflected in a clear reduction of the surface area of the SAM in scanning electron microscopy images, diminishing the visible area from around 400% to 200% compared to wild type (Fig. 5, D and E). As for the analysis of SAM sections, the impact of the *RAP2.6L-SX* transgene on the surface area of the SAM was only significant in the *amp1* mutant, but not in the wild-type background, indicating a specific genetic interaction between *RAP2.6L-SX* and *amp1*. Thus, perturbation of the function of RAP2.6L not only suppresses the increased true leaf production of the *amp1* mutant but also mitigates its abnormal SAM expansion phenotype.

RAP2.6L Mediates the Enhanced Shoot Regeneration Capacity of the *amp1* Mutant

RAP2.6L is required for shoot renewal in tissue culture (Che et al., 2006) and the *amp1* mutant shows a higher shoot-regenerative capacity (Chaudhury et al., 1993) as well as ectopic shoot stem cell marker expression in the root (Poretska et al., 2016). To determine whether increased expression of *RAP2.6L* contributes to the elevated de novo SAM formation in the *amp1* mutant, we also analyzed the impact of RAP2.6L deficiency on this process. As previously shown (Che et al., 2006), the *rap2.6l* mutant displayed diminished regeneration of shoots from root explants (Fig. 6, A and B). This defect was further pronounced in the *rap2.6l erf112* double mutant and in the *RAP2.6L-SX* transgenic plants, whereas this process was unaffected in the *erf112* mutant and the *EBE-SX* transgenic plants (Fig. 6, A and B). Intriguingly, overexpression of *RAP2.6L* in the wild type prominently promoted the shoot de novo formation capacity almost to the same extent as in the *amp1-1* mutant. Conversely, the presence of the *RAP2.6L-SX* transgene or the *rap2.6l erf112* mutation suppressed the elevated shoot regeneration of the *amp1* mutant to levels similar or even lower than in the wild type. Again here, the effect of the *rap2.6l* and *erf112* mutation and the presence of the *EBE-SX* transgene were much more subtle in this respect (Fig. 6, A and B). Together, these findings provide evidence that the upregulated expression of *RAP2.6L* in the *amp1* mutant contributes to its enhanced shoot regeneration capacity.

RAP2.6L Expression Is Controlled by HD-ZIP III Proteins

Next, we tried to establish how AMP1 impacts the expression of *RAP2.6L* at the molecular level. AMP1 is required for the translational inhibition of miRNA targets (Li et al., 2013). Therefore, enhanced activity of the miRNA-controlled components regulating the expression of *RAP2.6L* might cause its overexpression in the *amp1* mutant. We screened the Genevestigator expression database for genetic perturbations affecting the expression of *RAP2.6L* (Hruz et al., 2008). We detected highly elevated *RAP2.6L* mRNA levels in embryos of *dcl1*-15, a miRNA-biosynthesis-deficient mutant (Willmann et al., 2011), consistent with the assumption that *RAP2.6L* expression is under the control of a miRNA target (Supplemental Fig. S5A). Moreover, this analysis revealed that transcript levels of *RAP2.6L* are also increased in the *35S:GR-REV** plants (Supplemental Fig. S5B), a line bearing a chemically inducible, miRNA-resistant version of REVOLUTA (Reinhart et al., 2013), suggesting that HD-ZIP III transcription factors, which overaccumulate in the *amp1* mutant (Supplemental Fig. S6; Li et al., 2013; Poretska et al., 2016), might affect the expression of *RAP2.6L*. This was further supported by a significant up-regulation of *RAP2.6L* mRNA levels in mutants containing miRNA-resistant alleles of either *PHABULOSA* (*phb-1d*) or *REVOLUTA* (*rev-10d*; Fig. 7A). Similarly, overexpression of a yellow fluorescent protein (YFP)-tagged version of *PHAVOLUTA* (*PHV*) promoted the accumulation of *RAP2.6L* transcripts (Fig. 7A). To test whether the transcription of *RAP2.6L* is under direct control of HD-ZIP III proteins, we analyzed the *RAP2.6L* promoter region for the presence of described HD-ZIP III binding motifs. Although the 11-nucleotide inverted palindromic sequence identified by in vitro binding studies of PHV was not present (Sessa et al., 1998), we detected eight AT[G/C]AT repeats representing the inner core of this motif (Fig. 7B), which was defined as the cis-regulatory binding domain of REV based on chromatin immunoprecipitation (ChIP)-seq experiments (Brandt et al., 2012). To assess whether PHV directly binds to the *RAP2.6L* promoter in vivo, chromatin extracts from wild-type and *35S::PHV-YFP* seedlings were immunoprecipitated with an anti-YFP antibody. This analysis revealed that PHV-YFP is associated with two *RAP2.6L* promoter fragments containing two overlapping AT[G/C]AT repeats each (Fig. 7B). In line with a direct control of *RAP2.6L* transcription by HD-ZIP III proteins, we found an adaxial/central expression pattern of the pRAP2.6L::GUS reporter in late-stage embryos (Fig. 7C). Moreover, compared to the barely visible reporter activity in the wild type, the signal was strongly enhanced in the *amp1* mutant, supporting the model that enhanced HD-ZIP III activity in the *amp1* mutant drives the ectopic expression of *RAP2.6L*. In light of these data, we propose an emerging regulatory module for the control of SAM organization, in which AMP1 constricts stem cell pool homeostasis through limitation of the expression of *RAP2.6L* via translational control of HD-ZIP III activity.

DISCUSSION

The putative carboxypeptidase AMP1 has been identified as a crucial determinant of radial SAM organization by suppression of stem cell identity in the morphogenetic zone (Huang et al., 2015). The absence of AMP1 causes disorganized growth patterns and uncoordinated hyperproliferative organ formation in the shoot. Despite the developmental importance of this enzyme, neither its biochemical function nor the

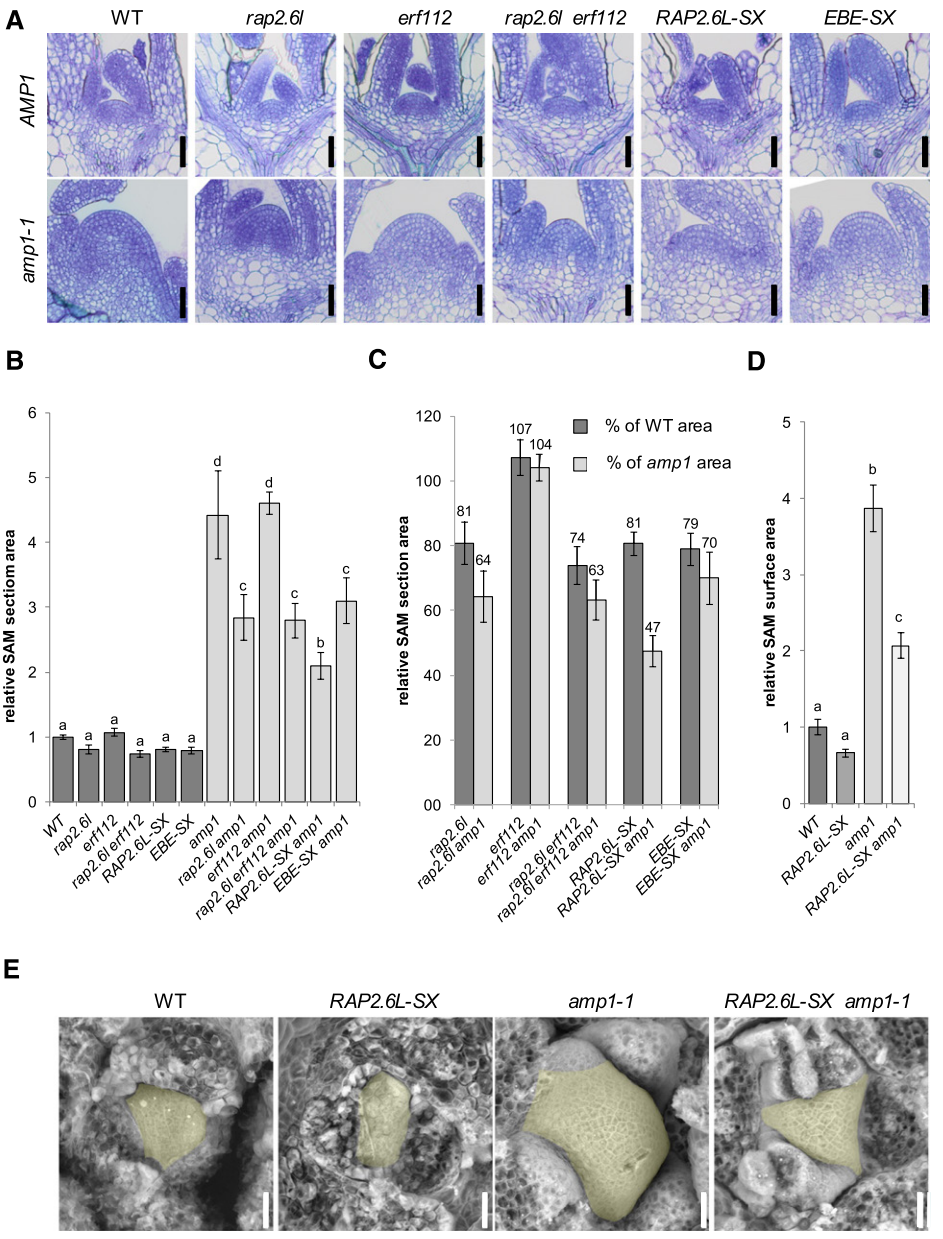

Figure 5. Compromised function of RAP2.6L affects SAM size in the *amp1* mutant. A, Median longitudinal SAM sections of wild-type Col-0 (WT), *rap2.6l-1*, *erf112-1*, *rap2.6l-1 erf112-1*, *RAP2.6L-SX*, and *EBE-SX* plants in the wild-type background at 7 DAG (top) and median longitudinal SAM sections of the same lines in the *amp1-1* background at 7 DAG (bottom). B, Quantification of the SAM area from median longitudinal sections of the indicated genotypes at 7 DAG (bars represent means ± SE; $n \geq 4$). The SAM areas were normalized to that of wild-type Col-0 (wild type = 1). Bars for plant lines in the wild-type background are colored in dark gray, and bars for lines in the *amp1-1* background are colored in light gray. Different letters over the error bars indicate significant differences ($P < 0.05$) as estimated by Duncan's multiple range test. C, Relative reduction of median SAM section areas by the indicated genotypes compared to wild-type Col-0 (WT) and the *amp1-1* mutant based on the data shown in B. Bars represent normalized values ± SE; $n \geq 4$. Normalized values are shown above the error bars. D, Quantification of SAM surface area from scanning electron micrographs of the indicated genotypes at 7 DAG (bars represent means ± SE; $n \geq 3$). The SAM areas were normalized to that of wild-type Col-0 (wild type = 1). Different letters over the error bars indicate significant differences ($P < 0.05$) as estimated by Duncan's multiple range test. E, Scanning electron micrographs of the SAM of wild-type Col-0 (WT), *RAP2.6L-SX*, *amp1-1*, and *RAP2.6L-SX amp1-1* seedlings. The SAM areas are highlighted in yellow. Bars = 25 µm (A and E).

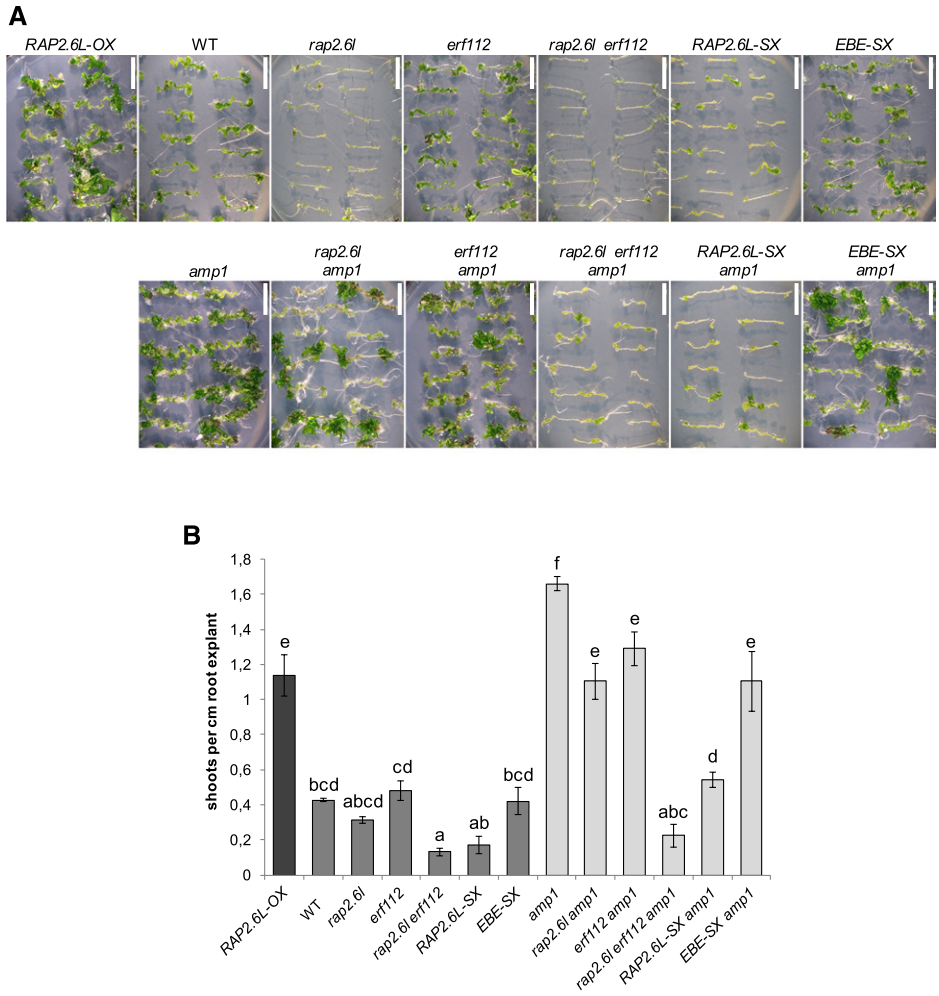

Figure 6. Compromised function of RAP2.6L affects shoot regeneration in the *amp1* mutant. A, Representative root explants of the indicated genotypes after 18 d on shoot induction medium. B, Quantification of shoot regeneration of the indicated genotypes. Bars for plant lines in the wild-type background are colored in dark gray, and bars for lines in the *amp1-1* background are colored in light gray. The regenerative capacity was calculated as the number of shoots/cm root explant (bars represent means ± SE; $n \geq 30$). Different letters over the error bars indicate significant differences ($P < 0.05$) as estimated by Duncan's multiple range test. Bars = 10 mm.

regulatory network by which AMP1 controls SAM organization is known. AMP1 limits the translation rate of a broad range of tested miRNA targets (Li et al., 2013). However, whether and how AMP1 controls SAM activity by this mechanism is still elusive. In this work, we showed that the AP2/ERF transcription factor RAP2.6L is strongly upregulated in the absence of AMP1 and that this up-regulation at least partially accounts for the observed phenotypic defects found in the mutant. Moreover, we provide evidence that the ectopic expression of *RAP2.6L* is driven by the enhanced translation of HD-ZIP III proteins in the *amp1* mutant. We propose with *RAP2.6L* a new regulatory node downstream of AMP1, important for shoot SCN specification.

A role of RAP2.6L in the determination of shoot stem cell identity is supported by earlier studies. RAP2.6L had originally been identified as an essential component of shoot regeneration, since its expression was strongly induced upon transfer of explants to shoot induction medium and its absence severely impaired shoot formation in tissue culture (Che et al., 2006). RAP2.6L is thus a crucial driver of transdifferentiation from root meristem-like callus to newly formed SAMs (Duclercq et al., 2011b). This function is also supported by the finding that upon wounding of inflorescence stems, the expression of *RAP2.6L* specifically increased at the lower side of the incision zone (Asahina et al., 2011), an area which under certain circumstances, such as shoot decapitation, gives rise to novel SAMs. Moreover, close homologs of RAP2.6L in the Xa group of the AP2/ERF transcription factor family were also shown to be involved in SCN establishment and recovery. Overexpression of *EBE/ERF114* not only caused

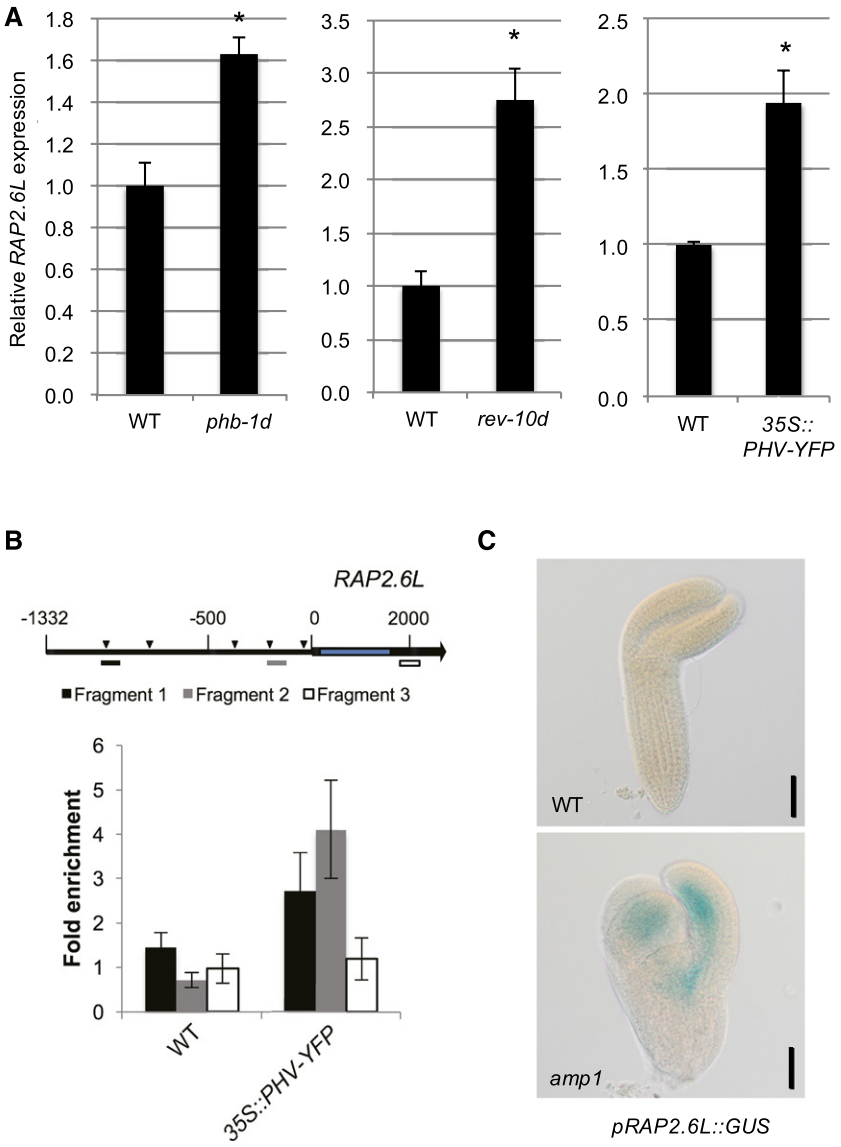

Figure 7. *RAP2.6L* expression is controlled by HD-ZIP III proteins. A, qPCR analysis of *RAP2.6L* expression in 10-d-old seedlings of *phb-1d* (left), *rev-10d* (middle), and *35S::PHV-YFP* (right) plants. Normalized means (wild type = 1) are shown. Error bars indicate the SE calculated from three biological replicates (at least 30 seedlings per replicate; replicates were grown at the same time on different petri dishes) after normalization to *UBC*. Asterisks indicate a significant difference (Student's two-tailed *t* test; $P < 0.05$). B, ChIP analysis using 35S::PHV-YFP seedlings. An illustration of the *RAP2.6L* genomic region is shown (top). The black arrow represents the *RAP2.6L* transcript region, and the intron region is shown in blue. The transcription start is labeled as 0. Triangles in the promoter region indicate the identified HD-ZIP III binding motifs (AT[G/C]AT). Positions of the genomic fragments analyzed in the ChIP experiment are indicated as differently colored bars. Enrichment of PHV-YFP at the *RAP2.6L* promoter was determined by qPCR and shown by the ratio between samples treated with antibody and samples treated without antibody. Error bars indicate the SE calculated from at least three biological replicates (around 500 seedlings per replicate; replicates were grown at the same time on different petri dishes). C, *pRAP2.6L::GUS* activity in wild-type (WT) and *amp1-1* embryos analyzed by differential interference contrast microscopy. Bars = 50 µm.

ectopic formation and enhanced outgrowth of axillary shoot meristems, but also increased the size and activity of the vegetative SAM (Mehrnia et al., 2013) similar to the effect of *RAP2.6L* overexpression described in this study. ERF115 displays an analogous role in the root meristem. Together with PHYTOCHROME A SIGNAL TRANSDUCTION1, ERF115 mediates SCN recovery from differentiated cells in the wounding zone of excised root meristems, and ubiquitous expression of the ERF115/PHYTOCHROME A SIGNAL TRANSDUCTION1 complex causes ectopic stem cell pool formation in the root (Heyman et al., 2016). ERF115 exerts

its regenerative capacity at least partially by activating the AP2 transcription factor WOUND INDUCED DEDIFFERENTIATION1, a key player in the wound-induced regeneration processes (Iwase et al., 2011; Heyman et al., 2016). It is still unknown if RAP2.6L also acts through WOUND INDUCED DEDIFFERENTIATION1 or other AP2/ERF proteins involved in shoot regeneration, such as PHLETHORA3/5/7 or ESR1/DRN and ESR2/DRNL.

In light of the phenotypic similarities between RAP2.6L and EBE/ERF114 gain-of-function lines, the question arises whether AMP1 mainly acts through RAP2.6L or also through other members of this ERF subfamily. Although only RAP2.6L among the tested homologs was significantly upregulated in the *amp1* mutant in whole-seedling expression analyses, we found that the *amp1* shoot defects were more strongly suppressed by the *rap2.6l erf112* mutation than by the *rap2.6l* mutation alone and were most efficiently abrogated by the presence of the *RAP2.6L-SX* transgene. The *RAP2.6L-SX* line might affect the activity of additional homologs acting on the same promoters based on its dominant-negative nature. Next to ERF112, RAP2.6 potentially cooperates with RAP2.6L to mediate *amp1*-related phenotypes, since its expression appeared to be slightly elevated in the *amp1* mutant background. Due to the missing suppressive effect of the *erf112* and *rap2.6* single mutations in the *amp1* background, in contrast to the *rap2.6l* mutation and the strong impact of the *RAP2.6L-SX* transgene, we postulate that RAP2.6L represents the main target but is functionally escorted by ERF112 and RAP2.6. In contrast, EBE did not show enhanced expression in any of the tested *amp1* alleles, and the *EBE-SX* transgene was much weaker (concerning SAM size) or inefficient (concerning leaf number and shoot regeneration) in suppressing *amp1*-related shoot phenotypes as compared to the *RAP2.6L-SX* transgene. Based on these data, it will be interesting to further investigate the specific interaction of ERF112, RAP2.6, and RAP2.6L in shoot SCN replenishment and their functional relationships with AMP1 in this process.

Since AMP1 has been recently positioned in the miRNA-dependent control of translation, we reasoned that the observed induction of *RAP2.6L* in the *amp1* mutant might be caused by excessive translation of miRNA targets affecting its expression. Correspondingly, we found enhanced expression of *RAP2.6L* in diverse Arabidopsis lines with increased activity of members of the miRNA-controlled family of HD-ZIP III transcription factors and showed that PHV is enriched on the RAP2.6L promoter *in vivo*. Consistent with a direct control of the expression of RAP2.6L by PHV, we also observed overlapping expression patterns in the embryo. HD-ZIP III transcription factors determine shoot meristem identity during embryogenesis (Smith and Long, 2010), and proper control of their activity is important to maintain the radial symmetry of the SAM (Green et al., 2005; Williams et al., 2005; Kim et al., 2008), making it plausible that their enhanced translation in the *amp1* mutant (Li et al., 2013; Poretska et al., 2016) contributes to the ectopic SCN formation. Notably, the enhanced posttranslational activity of HD-ZIP IIIs in the *zpr3 zpr4* double mutant provokes the ring-like expansion of the shoot SCN in young seedlings, which is highly reminiscent of what is found in strong *amp1* alleles (Kim et al., 2008; Huang et al., 2015). How HD-ZIP III proteins determine shoot meristem identity at the mechanistic level is not well understood, but recent studies revealed a direct impact on key factors such as WUS (Zhang et al., 2017). With RAP2.6L, we identified an additional component acting downstream of HD-ZIP III in the control of shoot meristem patterning. Future genetic analysis should further dissect the functional relevance of this interaction.

Since AMP1 affects the translation of a broad range of tested miRNA targets (Li et al., 2013), the HD-ZIP III/RAP2.6L regulatory cascade is most likely not the only avenue by which AMP1 affects SAM organization. This might be one reason why ectopic expression of *RAP2.6L* does not fully mimic the *amp1* shoot phenotype. Moreover, the enhanced translation of HD-ZIP IIIs in the *amp1* mutant potentially misregulates other key determinants of SAM organization such as WUS, which has recently been shown to be under transcriptional control of REV/PHB/PHV in the process of shoot regeneration (Zhang et al., 2017). Nevertheless, the strong suppressive effect of the *RAP2.6L-SX* transgene on the overall SAM activity of the *amp1* mutant shown in this study, compared to the obvious genetic epistasis of *amp1* over *wus* (Huang et al., 2015), supports a prominent role of RAP2.6L downstream of AMP1. Furthermore, a specific functional interaction between AMP1 and HD-ZIP III proteins is supported by the finding that the expression of *AMP1* is regulated by REV (Reinhart et al., 2013), potentially representing a negative feedback control mechanism.

We cannot fully exclude the existence of HD-ZIP III-independent modes of *RAP2.6L* activation in the *amp1* mutant. Whereas direct induction by the increased cytokinin levels in the *amp1* mutant appears rather unlikely based on the unresponsiveness of *RAP2.6L* transcription toward exogenous cytokinin application (Supplemental Fig. S2; Che et al., 2006), induction might be caused by the enhanced jasmonic acid (JA) response found in the *amp1* mutant (Poretska et al., 2016). *RAP2.6L* expression is promoted upon application of JA, a hormone synthesized upon wounding. Interestingly, wounding has been shown to be important for the regeneration processes. However, how wounding triggers regeneration at the molecular level and the specific role of JA in this process are not well understood (Ikeuchi et al., 2016). Whether the altered JA response in the *amp1* mutant is functionally relevant with respect to the defect in SAM organization and the elevated transcript levels of *RAP2.6L* are important future questions to be resolved.

Finally, it remains unclear how enhanced *RAP2.6L* expression in *amp1* triggers the expansion of SCN identity in the peripheral zone of the meristem as

well as the enhanced ability for shoot regeneration in root explants. A potential downstream component is CUP-SHAPED COTYLEDON2, a transcription factor required for embryonic SAM formation and shoot regeneration in tissue culture, whose expression has been shown to depend on RAP2.6L (Che et al., 2006). Another future research direction might be to analyze whether RAP2.6L feeds back on HD-ZIP III activity by physical interaction. The AP2/ERF transcription factors ESR1/DRN and ESR2/DRNL bind to HD-ZIP IIIs and cooperate in shoot patterning during embryogenesis (Chandler et al., 2007). It will be interesting to see whether RAP2.6L has a related competence to modulate HD-ZIP III function in the control of SAM development.

MATERIALS AND METHODS

Plant Materials and Growth Conditions

Arabidopsis (*Arabidopsis thaliana*) ecotypes Columbia (Col-0) and Landsberg erecta (L*er*) were used in this study. *amp1-1* (Col-0; N8324), *amp1-13* (Col-0; N522988), *pt* (L*er*; N235), *lamp1-2* (Col-0; SM_3.22750), *rap2.6-2* (N863006), *rap2.6l-1* (N656482), *erf112-1* (N563727), and *phb-1d* (N3761) were ordered from the Nottingham Arabidopsis Stock Centre (http://www.arabidopsis.info), and genotypes of *rap2.6-2*, *rap2.6l-1*, and *erf112-1* were verified by PCR genotyping (Supplemental Fig. S7). *35S::PHV-YFP* was described previously (Poretska et al., 2016). The *35S::RAP2.6L* lines (C23, C28, and C31; named *RAP2.6L-OX* throughout this study) and *pRAP2.6L::RAP2.6L:GUS* were kindly provided by Nat Kav (Krishnaswamy et al., 2011). Of the RAP2.6L overexpression lines, C28 was used throughout this study unless indicated otherwise. *rev-10d* was obtained from Stephan Wenkel. *CycB1;1::CycB1;1-GUS* (in Col-0) was provided by John Celenza (DiDonato et al., 2004), *pCLV3::GUS*, and *pWUS::GUS* (in L*er*) were received from Thomas Laux (Gross-Hardt et al., 2002), and *pKLU::GUS* (in Col-0) was donated by Michael Lenhard (Anastasiou et al., 2007). Combinations of mutants and reporter lines were generated by crossing individual lines, and genotypes were verified phenotypically and by PCR genotyping (see primers in Supplemental Table S1).

Arabidopsis seeds were surface sterilized with 70% ethanol containing 0.05% SDS for 3 min and rinsed with 96% ethanol for 1 min.

The seeds were plated on half-strength Murashige and Skoog (MS) medium (Duchefa) containing 0.7% (w/v) agar (Duchefa) and 1% (w/v) Suc or in soil. After stratification (4°C for 48 h), seeds were transferred to the incubator set to long-day conditions (16 h of 80 µmol s^{-1} m^{-2} light/8 h dark) or short-day conditions (8 h of 80 µmol s^{-1} m^{-2} light/16 h dark). For the hyperphyllin treatment, seeds were germinated in liquid half-strength MS medium containing 1% (w/v) Suc in the presence or absence of the drug and analyzed at 10 DAG.

Gene Constructs and Transformation

PCR was performed with proofreading thermostable polymerase (Thermo Fisher Scientific), and all clones were confirmed by sequencing. To create 35S::RAP2.6L-MYC-SRDX (RAP2.6L-SX) and 35S::EBE-MYC-SRDX (EBE-SX), the RAP2.6L and EBE ORFs were amplified from cDNA (Col-0) by PCR with the primer pairs RAP2.6L ORF F (*Eco*RV)/RAP2.6L ORF R (*Not*I) and EBE ORF F (*Eco*RV)/EBE ORF R (*Not*I), respectively. The fragment was subcloned into pGEM-T Easy (Promega). Subsequently, in a previously created pGWR8-CES-MYC-SRDX (Poppenberger et al., 2011), the CES ORF was removed by a double digestion with *Eco*RV and *Not*I to generate the pGWR8-MYC-SRDX backbone. The RAP2.6L and EBE ORFs were then transferred via *Eco*RV and *Not*I into pGWR8-MYC-SRDX to generate RAP2.6L-SX and EBE-SX, respectively.

To create pRAP2.6L::GUS, a 1,487-bp genomic sequence upstream of the RAP2.6L ORF was amplified with primers AP2.6proF(*Pst*I) and AP2.6pro-R(*Bam*HI) and subcloned into pGEM-T Easy (Promega). The fragment was excised using *Pst*I and *Bam*HI and ligated into pPZP-GUS-1 (Diener et al., 2000), resulting in pRAP2.6L::GUS.

Plants were transformed using the floral-dip method, at least 10 independent transformants were generated for each line, and the resulting T2 lines were confirmed for single transgene insertion sites based on the 3:1 segregation of the selection marker and propagated for further analysis.

GUS Staining

Seedlings were put into the freshly made GUS staining buffer (100 mM sodium phosphate buffer, 10 mM EDTA, 0.5 mM $K_3Fe(CN)_6$, 0.5 mM $K_4Fe(CN)_6$, Triton X-100 [0.1% v/v], and 1 mM 5-bromo-4-chloro-3-indolyl-β-D-glucuronide). The seedlings were incubated at 37°C for a duration of time depending on the reporter strength. After staining, the seedlings were dehydrated with 70% ethanol. Seedlings were analyzed using a stereomicroscope (SZX10; Olympus) equipped with a digital camera (DP26; Olympus).

Histology

The histological analysis was performed as previously described (De Smet et al., 2004). Seedlings were grown under long-day conditions for 8 d or short-day conditions for 18 d and fixed overnight at 4°C in formaldehyde-acetic acid-alcohol (5% [v/v] formaldehyde, 5% [v/v] acetic acid, and 50% [v/v] ethanol). After fixation, samples were dehydrated in a graded ethanol series (2 h each in 30%, 50%, 70%, and 96% ethanol) and embedded with Technovit 7100 (Heraus Kulzer) according to the manufacturer's instructions. A series of 5- to 7-µm-thick longitudinal sections was made with a Leica RM 2065 microtome. Sections were transferred to microscopic slides (Marienfeld), stained for 5 min in 0.02% aqueous Toluidine blue O (Sigma-Aldrich), and rinsed with water. Subsequently, the stained sections were analyzed with a microscope (BX-61; Olympus).

Scanning Electron Microscopy

Seedlings were fixed in formaldehyde-acetic acid-alcohol (50% ethanol, 10% acetic acid, and 5% formaldehyde) overnight at 4°C and then dehydrated through a graded ethanol series up to 96% ethanol and supercritical point-dried (CPD300; Leica Microsystems). Dried seedlings were dissected and mounted on conductive adhesive tabs (PLANO) under a stereomicroscope (SZX10; Olympus). Samples were subsequently examined using a T-3000 tabletop scanning electron microscope (Hitachi).

Leaf Number Analysis

The shoot apex area of seedlings was examined under the stereomicroscope (2× magnification) at the indicated developmental stages and the number of visible leaves was recorded.

Regeneration Capacity Assay

The regeneration capacity assay was performed based on a previous protocol (Che et al., 2006). In brief, Arabidopsis seedlings were grown for 7 d on 0.5× MS medium under long-day conditions. Root segments of 1 to 1.5 cm were cut, transferred to Gamborg's B5 medium (Sigma-Aldrich) supplemented with 0.5 g/L MES (pH set to 5.7 with KOH), 2.2 µM 2,4-dichlorophenoxyacetic acid, 0.2 µM kinetin, and 0.8% agarose (callus induction medium), and incubated under constant light for 4 d. The root explants were then transferred to shoot induction medium (Gamborg's B5 medium containing 0.5 g/L MES [pH set to 5.7 with KOH], 5.0 µM isopentenyladenine, 0.9 µM indole acetic acid, and 0.8% agarose) and incubated under constant light for 18 d. Regenerated shoots were counted and the number of regenerated shoots per cm explant was calculated.

Reverse Transcription-qPCR

About 50 mg of seedling material was collected, shock-frozen in liquid nitrogen, and homogenized with a Retsch mill (Verder Scientific). The total RNA was extracted with the E.N.Z.A. Plant RNA Mini Kit (OMEGA Bio-Tek) and

treated with DNase I (Thermo Fisher Scientific). The first-strand cDNA was synthesized using the extracted RNA as template with the RevertAid first-strand cDNA synthesis kit (Thermo Fisher Scientific). qPCR was performed with an Eppendorf Realplex Mastercycler using SensiFAST SYBR Lo-ROX Mix (Bioline) and specific primers (Supplemental Table S1) for the mRNAs of interest. Data were normalized to *UBC* (*AT5G25760*) and measured in at least three technical replicates.

Western Blotting

Western blotting was performed as previously described (Poretska et al., 2016).

ChIP Assays

One gram of 10-d-old plants was submerged in 1% formaldehyde solution, and a vacuum was applied for 10 min. Cross linking was quenched by adding 125 mM Gly, and a vacuum was applied for 5 min. After rinsing two times with double-distilled water, the plant material was ground to a fine powder in liquid nitrogen, and chromatin preparation was performed as previously described (Poppenberger et al., 2011). For immunoprecipitation, anti-GFP VHH agarose beads (Chromotek) and agarose beads as control were used. Washing of the beads and elution of the DNA-protein complex were performed as described previously (Kaufmann et al., 2010). DNA purification was performed with the MinElute PCR purification kit (Qiagen, Venlo, NL). For qPCR analysis, primers specific for the desired promoter region (listed in Supplemental Table S1) were used. Purified DNA fragments were used for establishing standard curves for quantification.

Accession Numbers

Sequence data from this article can be found in the GenBank data library under accession numbers AT3G54720 (AMP1), AT5G19740 (LAMP1), AT5G13330 (RAP2.6L), AT1G43160 (RAP2.6), AT2G33710 (ERF112), AT5G61890 (EBE), AT5G07310 (ERF115), AT5G25760 (UBC), AT2G34710 (PHB), AT5G60690 (REV), AT2G17950 (WUS), AT2G27250 (CLV3), AT1G13710 (KLU), and AT4G37490 (CYCB1;1).

Supplemental Data

The following supplemental materials are available.

Supplemental Figure S1. Expression analysis of ERF transcription factors closely related to *RAP2.6L*.

Supplemental Figure S2. *RAP2.6L* expression is not affected by cytokinin.

Supplemental Figure S3. Effect of compromised *RAP2.6* function on the leaf formation rate and shoot regeneration.

Supplemental Figure S4. Effect of compromised *RAP2.6L* function on the leaf formation rate of the *amp1* mutant.

Supplemental Figure S5. Expression of *RAP2.6L* is increased in the *dcl1* mutant and the *35S::GR-REV** transgenic plants.

Supplemental Figure S6. PHV::YFP overaccumulates in the *amp1* and *amp1 lamp1* mutants.

Supplemental Figure S7. Genotyping of the *rap2.6-2*, *rap2.6l-1*, and *erf112-1* mutants.

Supplemental Table S1. List of oligos used in this study.

ACKNOWLEDGMENTS

We thank John Chelenza, Nat Kav, Thomas Laux, Michael Lenhard, and Stephan Wenkel for providing published material. We thank Pablo Albertos, Brigitte Poppenberger, and Wilfried Rozhon for critical reading of the manuscript. We also thank Julius Mayer for helping with SAM sectioning and Irene Ziegler for technical assistance.

Received February 28, 2018; accepted May 29, 2018; published June 8, 2018.

LITERATURE CITED

Anastasiou E, Kenz S, Gerstung M, MacLean D, Timmer J, Fleck C, Lenhard M (2007) Control of plant organ size by KLUH/CYP78A5-dependent intercellular signaling. Dev Cell **13**: 843–856

Asahina M, Azuma K, Pitaksaringkarn W, Yamazaki T, Mitsuda N, Ohme-Takagi M, Yamaguchi S, Kamiya Y, Okada K, Nishimura T, (2011) Spatially selective hormonal control of RAP2.6L and ANAC071 transcription factors involved in tissue reunion in Arabidopsis. Proc Natl Acad Sci USA **108**: 16128–16132

Banno H, Ikeda Y, Niu QW, Chua NH (2001) Overexpression of Arabidopsis ESR1 induces initiation of shoot regeneration. Plant Cell **13**: 2609–2618

Brand U, Fletcher JC, Hobe M, Meyerowitz EM, Simon R (2000) Dependence of stem cell fate in Arabidopsis on a feedback loop regulated by CLV3 activity. Science **289**: 617–619

Brandt R, Salla-Martret M, Bou-Torrent J, Musielak T, Stahl M, Lanz C, Ott F, Schmid M, Greb T, Schwarz M, (2012) Genome-wide binding-site analysis of REVOLUTA reveals a link between leaf patterning and light-mediated growth responses. Plant J **72**: 31–42

Chandler JW, Cole M, Flier A, Grewe B, Werr W (2007) The AP2 transcription factors DORNROSCHEN and DORNROSCHEN-LIKE redundantly control Arabidopsis embryo patterning via interaction with PHAVOLUTA. Development **134**: 1653–1662

Chaudhury AM, Letham S, Craig S, Dennis ES (1993) Amp**1**: a mutant with high cytokinin levels and altered embryonic pattern, faster vegetative growth, constitutive photomorphogenesis and precocious flowering. Plant J **4**: 907–916

Che P, Lall S, Nettleton D, Howell SH (2006) Gene expression programs during shoot, root, and callus development in Arabidopsis tissue culture. Plant Physiol **141**: 620–637

Chickarmane VS, Gordon SP, Tarr PT, Heisler MG, Meyerowitz EM (2012) Cytokinin signaling as a positional cue for patterning the apical-basal axis of the growing Arabidopsis shoot meristem. Proc Natl Acad Sci USA **109**: 4002–4007

Daum G, Medzihradszky A, Suzaki T, Lohmann JU (2014) A mechanistic framework for noncell autonomous stem cell induction in Arabidopsis. Proc Natl Acad Sci USA **111**: 14619–14624

De Smet I, Chaerle P, Vanneste S, De Rycke R, Inzé D, Beeckman T (2004) An easy and versatile embedding method for transverse sections. J Microsc **213**: 76–80 10.1111/j.1365-2818.2004.01269.x14678515

DiDonato RJ, Arbuckle E, Buker S, Sheets J, Tobar J, Totong R, Grisafi P, Fink GR, Celenza JL (2004) Arabidopsis ALF4 encodes a nuclear-localized protein required for lateral root formation. Plant J **37**: 340–353

Diener AC, Li H, Zhou W, Whoriskey WJ, Nes WD, Fink GR (2000) Sterol methyltransferase 1 controls the level of cholesterol in plants. Plant Cell **12**: 853–870 10.1105/tpc.12.6.85310852933

Duclercq J, Assoumou Ndong YP, Guerineau F, Sangwan RS, Catterou M (2011a) Arabidopsis shoot organogenesis is enhanced by an amino acid change in the ATHB15 transcription factor. Plant Biol (Stuttg) **13**: 317–324

Duclercq J, Sangwan-Norreel B, Catterou M, Sangwan RS (2011b) De novo shoot organogenesis: from art to science. Trends Plant Sci **16**: 597–606

Gaillochet C, Lohmann JU (2015) The never-ending story: from pluripotency to plant developmental plasticity. Development **142**: 2237–2249

Gordon SP, Chickarmane VS, Ohno C, Meyerowitz EM (2009) Multiple feedback loops through cytokinin signaling control stem cell number within the Arabidopsis shoot meristem. Proc Natl Acad Sci USA **106**: 16529–16534

Green KA, Prigge MJ, Katzman RB, Clark SE (2005) CORONA, a member of the class III homeodomain leucine zipper gene family in Arabidopsis, regulates stem cell specification and organogenesis. Plant Cell **17**: 691–704

Griffiths J, Barrero JM, Taylor J, Helliwell CA, Gubler F (2011) ALTERED MERISTEM PROGRAM 1 is involved in development of seed dormancy in Arabidopsis. PLoS One **6**: e20408

Gross-Hardt R, Lenhard M, Laux T (2002) WUSCHEL signaling functions in interregional communication during Arabidopsis ovule development. Genes Dev **16**: 1129–1138

Helliwell CA, Chin-Atkins AN, Wilson IW, Chapple R, Dennis ES, Chaudhury A (2001) The Arabidopsis AMP1 gene encodes a putative glutamate carboxypeptidase. Plant Cell **13**: 2115–2125

Heyman J, Cools T, Canher B, Shavialenka S, Traas J, Vercauteren I, Van den Daele H, Persiau G, De Jaeger G, Sugimoto K, (2016) The heterodimeric transcription factor complex ERF115-PAT1 grants regeneration competence. Nat Plants **2**: 16165

Hruz T, Laule O, Szabo G, Wessendorp F, Bleuler S, Oertle L, Widmayer P, Gruissem W, Zimmermann P (2008) Genevestigator v**3**: a reference expression database for the meta-analysis of transcriptomes. Adv Bioinforma **2008**: 420747

Huang W, Pitorre D, Poretska O, Marizzi C, Winter N, Poppenberger B, Sieberer T (2015) ALTERED MERISTEM PROGRAM1 suppresses ectopic stem cell niche formation in the shoot apical meristem in a largely cytokinin-independent manner. Plant Physiol **167**: 1471–1486

Ikeuchi M, Ogawa Y, Iwase A, Sugimoto K (2016) Plant regeneration: cellular origins and molecular mechanisms. Development **143**: 1442–1451

Iwase A, Mitsuda N, Koyama T, Hiratsu K, Kojima M, Arai T, Inoue Y, Seki M, Sakakibara H, Sugimoto K, (2011) The AP2/ERF transcription factor WIND1 controls cell dedifferentiation in Arabidopsis. Curr Biol **21**: 508–514

Je BI, Gruel J, Lee YK, Bommert P, Arevalo ED, Eveland AL, Wu Q, Goldshmidt A, Meeley R, Bartlett M, (2016) Signaling from maize organ primordia via FASCIATED EAR3 regulates stem cell proliferation and yield traits. Nat Genet **48**: 785–791

Kareem A, Radhakrishnan D, Sondhi Y, Aiyaz M, Roy MV, Sugimoto K, Prasad K (2016) De novo assembly of plant body plan: a step ahead of Deadpool. Regeneration (Oxf) **3**: 182–197

Kaufmann K, Muiño JM, Østerås M, Farinelli L, Krajewski P, Angenent GC (2010) Chromatin immunoprecipitation (ChIP) of plant transcription factors followed by sequencing (ChIP-SEQ) or hybridization to whole genome arrays (ChIP-CHIP). Nat Protoc **5**: 457–472

Kim YS, Kim SG, Lee M, Lee I, Park HY, Seo PJ, Jung JH, Kwon EJ, Suh SW, Paek KH, (2008) HD-ZIP III activity is modulated by competitive inhibitors via a feedback loop in Arabidopsis shoot apical meristem development. Plant Cell **20**: 920–933

Krishnaswamy S, Verma S, Rahman MH, Kav NN (2011) Functional characterization of four APETALA2-family genes (RAP2.6, RAP2.6L, DREB19 and DREB26) in Arabidopsis. Plant Mol Biol **75**: 107–127

Li S, Liu L, Zhuang X, Yu Y, Liu X, Cui X, Ji L, Pan Z, Cao X, Mo B, (2013) MicroRNAs inhibit the translation of target mRNAs on the endoplasmic reticulum in Arabidopsis. Cell **153**: 562–574

Loiseau JE (1959) Observations et experimentation sur la phyllotaxie et le fonctionnement du sommet vegetatif chez quelques Balsaminacees. Ann Sci Nat Bot **11**: 1–214

Magnani E, Barton MK (2011) A per-ARNT-sim-like sensor domain uniquely regulates the activity of the homeodomain leucine zipper transcription factor REVOLUTA in Arabidopsis. Plant Cell **23**: 567–582

Matsuo N, Makino M, Banno H (2011) Arabidopsis ENHANCER OF SHOOT REGENERATION (ESR)1 and ESR2 regulate in vitro shoot regeneration and their expressions are differentially regulated. Plant Sci **181**: 39–46

Mayer KF, Schoof H, Haecker A, Lenhard M, Jürgens G, Laux T (1998) Role of WUSCHEL in regulating stem cell fate in the Arabidopsis shoot meristem. Cell **95**: 805–815

Mehrnia M, Balazadeh S, Zanor MI, Mueller-Roeber B (2013) EBE, an AP2/ERF transcription factor highly expressed in proliferating cells, affects shoot architecture in Arabidopsis. Plant Physiol **162**: 842–857

Nogué F, Hocart C, Letham DS, Dennis ES, Chaudhury AM (2000) Cytokinin synthesis is higher in the Arabidopsis amp1 mutant. Plant Growth Regul **32**: 267–273

Poppenberger B, Rozhon W, Khan M, Husar S, Adam G, Luschnig C, Fujioka S, Sieberer T (2011) CESTA, a positive regulator of brassinosteroid biosynthesis. EMBO J **30**: 1149–1161

Poretska O, Yang S, Pitorre D, Rozhon W, Zwerger K, Uribe MC, May S, McCourt P, Poppenberger B, Sieberer T (2016) The small molecule hyperphyllin enhances leaf formation rate and mimics shoot meristem integrity defects associated with AMP1 deficiency. Plant Physiol **171**: 1277–1290

Reinhardt D, Frenz M, Mandel T, Kuhlemeier C (2003) Microsurgical and laser ablation analysis of interactions between the zones and layers of the tomato shoot apical meristem. Development **130**: 4073–4083

Reinhart BJ, Liu T, Newell NR, Magnani E, Huang T, Kerstetter R, Michaels S, Barton MK (2013) Establishing a framework for the Ad/abaxial regulatory network of Arabidopsis: ascertaining targets of class III homeodomain leucine zipper and KANADI regulation. Plant Cell **25**: 3228–3249

Roodbarkelari F, Groot EP (2017) Regulatory function of homeodomain-leucine zipper (HD-ZIP) family proteins during embryogenesis. New Phytol **213**: 95–104

Schoof H, Lenhard M, Haecker A, Mayer KF, Jürgens G, Laux T (2000) The stem cell population of Arabidopsis shoot meristems in maintained by a regulatory loop between the CLAVATA and WUSCHEL genes. Cell **100**: 635–644

Sessa G, Steindler C, Morelli G, Ruberti I (1998) The Arabidopsis Athb-8, -9 and -14 genes are members of a small gene family coding for highly related HD-ZIP proteins. Plant Mol Biol **38**: 609–622

Sluis A, Hake S (2015) Organogenesis in plants: initiation and elaboration of leaves. Trends Genet **31**: 300–306

Smith ZR, Long JA (2010) Control of Arabidopsis apical-basal embryo polarity by antagonistic transcription factors. Nature **464**: 423–426

Vidaurre DP, Ploense S, Krogan NT, Berleth T (2007) AMP1 and MP antagonistically regulate embryo and meristem development in Arabidopsis. Development **134**: 2561–2567

Wang JW, Schwab R, Czech B, Mica E, Weigel D (2008) Dual effects of miR156-targeted SPL genes and CYP78A5/KLUH on plastochron length and organ size in *Arabidopsis thaliana*. Plant Cell **20**: 1231–1243

Williams L, Grigg SP, Xie M, Christensen S, Fletcher JC (2005) Regulation of Arabidopsis shoot apical meristem and lateral organ formation by microRNA miR166g and its AtHD-ZIP target genes. Development **132**: 3657–3668

Willmann MR, Mehalick AJ, Packer RL, Jenik PD (2011) MicroRNAs regulate the timing of embryo maturation in Arabidopsis. Plant Physiol **155**: 1871–1884

Yadav RK, Perales M, Gruel J, Girke T, Jönsson H, Reddy GV (2011) WUSCHEL protein movement mediates stem cell homeostasis in the Arabidopsis shoot apex. Genes Dev **25**: 2025–2030

Zhang TQ, Lian H, Zhou CM, Xu L, Jiao Y, Wang JW (2017) A two-step model for de novo activation of *WUSCHEL* during plant shoot regeneration. Plant Cell **29**: 1073–1087